Korean J. Chem. Eng., **25**(5), 1208-1211 (2008)

Fracture behavior of carbon/epoxy laminated composite reinforced by iron powder

Heekyu Choi*,†, Hao Huang, Dong-Uk Kim**, and Chee-Ryong Joe****

*School of Nano & Advanced Materials Engineering, Changwon National University,
9 Sarim-dong, Changwon, Gyeongnam 641-773, Korea
**Department of Mechanical Design and Manufacturing, Changwon National University,
9 Sarim-dong, Changwon, Gyeongnam 641-773, Korea
(*Received 8 January 2008 • accepted 1 March 2008*)

Abstract−The fracture behaviors of a newly developed iron-powder reinforced carbon/epoxy laminated composite are investigated in this paper. Three kinds of DCB (double cantilever beam) specimens (without iron powder, with iron powder and with iron powder in a magnetic field) were prepared by the ASTM D 5528-94a. For the third DCB specimen, the unidirectional laminas were stacked with iron powder spread evenly on each lamina's surface. This process was performed in a magnetic field to keep the iron powder standing along the out-plane direction. From the test data of Instron 5567, the fracture toughness, G_I, was calculated by using the compliance calibration method for each of the three kinds of specimens. The calculated fracture toughness shows that the iron powder effectively disturbs the progress of fiber branching between the laminates and provides a good stitching to the in-plane laminates during the fracture.

Key words: Powder Technology, Composite Materials, Iron Powder, Carbon/Epoxy Composite

INTRODUCTION

It is well known that carbon/epoxy laminated composites have a very high in-plane strength and stiffness. However, the weak out-plane strength makes them vulnerable to delamination. One of the most effective methods to increase the inter-laminar fracture toughness is through-thickness stitching, which has received considerable interest from many researchers. Cox et al. [1] investigated the delamination behavior of carbon z-fiber (short rods) through-thickness reinforced Carbon-Epoxy composite. It was found that the z-fibers effectively bridged the cracks and reduced the driving force for crack growth. Hwang and Shen [2] measured the opening-mode fracture toughness of interplay hybrid composite materials and stated that interplay hybrid composites have higher inter-laminar fracture toughness than single-fiber composites. Sankar et al. [3] reinforced the graphite/epoxy DCB(double cantilever beam) specimens with Kevlar stitching. And they concluded that the fracture toughness of the stitched graphite/epoxy specimens was found to be about 60 times that of an unstitched specimen. In general, these stitching methods all gave good solutions to reinforce the composite inter-laminar, although the stitching processes seemed complicated and costly.

In this paper, a new composite, iron-powder reinforced Carbon/Epoxy laminated composite will be introduced [4]. During the stacking process, the iron powder was conformed in the out plane by exploiting a magnetic field. DCB tests were conducted to investigate the fracture toughness of this new composite. It was found that the iron powder provides good stitching to the carbon/epoxy laminates.

EXPERIMENT

1. Iron Powder

Fig. 1 shows the SEM photograph of iron powder as experimental sample. The particle shape of iron powder of 500 μm was irregular and blocky. In this study, the unidirectional laminas were stacked with iron powder spread evenly on each lamina's surface. This process was performed in a magnetic field to keep the iron powder standing along the out-plane direction. It has good crack-resistance because the particle thread length along the Z-direction is longer than without the magnetic field. These improvements are found to be dependent on the particle thread type, thread diameter and the thread density.

2. Preparation of Specimen

Three types of DCB specimens were manufactured by hand laid-up and cured in an autoclave. The prepreg used was a USN 175B from SK Chemical Co. The material properties for the unidirectional lamina were: thickness 0.171 mm; weight 261 g/m^2; tensile strength 450 kgf/mm^2; tensile modulus 24,000 kgf/mm^2; fiber density 1.77 g/cm^3; and resin density 1.2 g/cm^3 (Provided by the manufacturer).

(1) Specimen #1: Carbon/epoxy laminated specimen without iron powder. This specimen was just stacked with 30 plies of unidirectional prepregs.

(2) Specimen #2: Carbon/epoxy laminated specimen with iron powder. For preparing this specimen, 30 plies of unidirectional lamina were stacked with iron powder spread evenly on each lamina surface. The iron powder (Fe=55.85) was manufactured by SAMCHUN PURE CHEMICAL CO., LTD.

(3) Specimen #3: Carbon/epoxy laminated specimen with iron powder and stacked in a magnetic field. The prepregs were laid directly on the magnet. The iron powder spread on each prepreg stood in an out-plane direction with the help of the magnetic force.

For all three specimens, 'teflon film' was inserted between the 15th and 16th plies during lay-up to form an initiation site for delamination. The laminates were bagged and cured in an autoclave from United McGill Corporation. A two-stage curing cycle was executed. In the first stage, the temperature was increased at a rate

†To whom correspondence should be addressed.
E-mail: hkchoi99@changwon.ac.kr

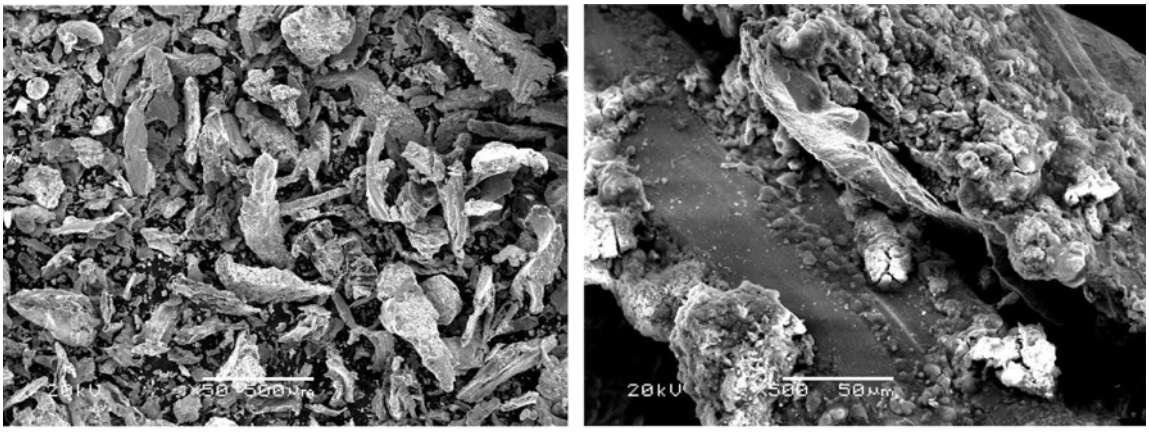

Fig. 1. Scanning electron microscopy (SEM) images showing the iron power as raw sample of this experiment. (a) ×50, (b) ×500.

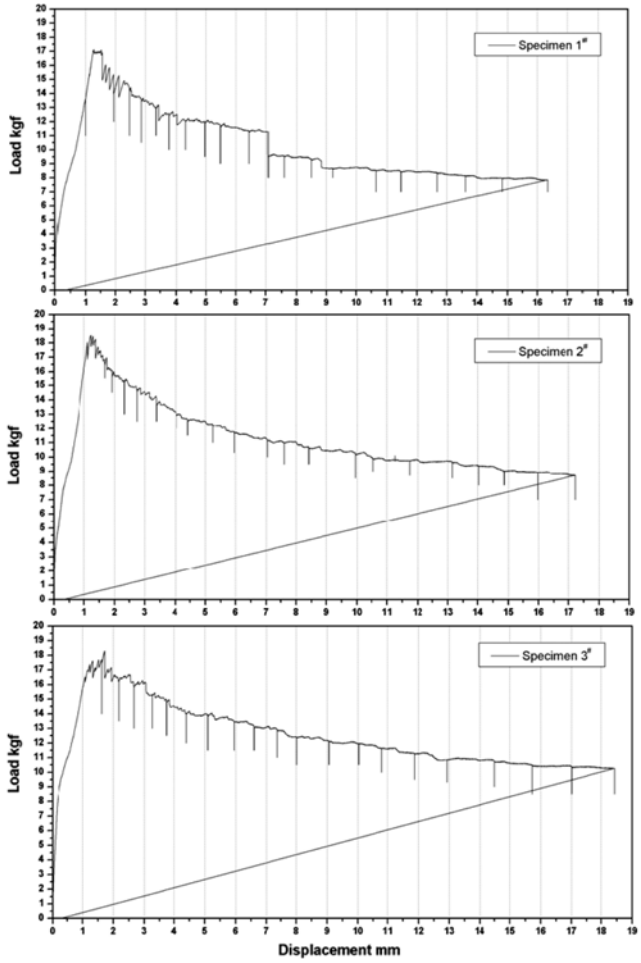

Fig. 2. Load-Displacement graph of Specimen #1-#3.

of 3 ℃/min from room temperature to 90 ℃. At the same time the pressure was increased to 0.55 MPa. In the second stage, the temperature was increased from 90 ℃ to 127 ℃ with 0.55 MPa.

The DCB specimens were cut from the laminates by using a diamond saw, and piano hinges were bonded to the both sides of the specimens. Before the test, the free edges of the specimen were paint-

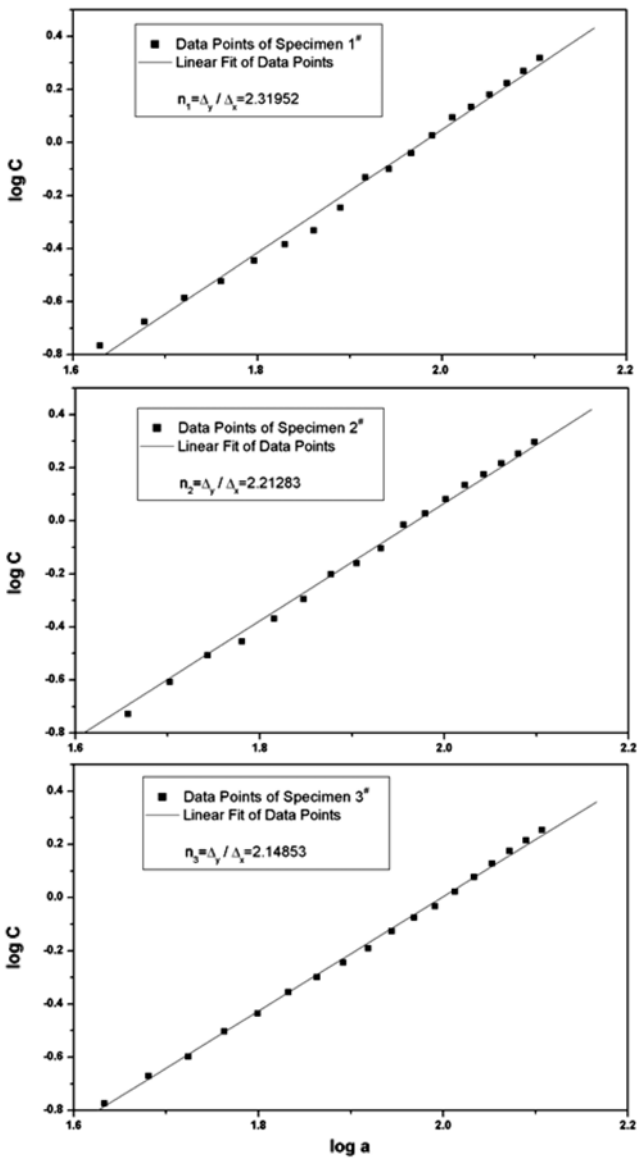

Fig. 3. Linear fitting of compliance vs. crack length for Specimen #1-#3.

ed with a white pen and clear lines were marked in the paint every 5 mm.

3. Description of Testing Procedure

The testing was conducted on an Instron 5567. The crosshead speed was 0.5 mm/min according to the ASTM D 5528-94a. An optical microscope was set up to observe the motion of the delamination front. Loading was forced to stop when crack propagation reached every 5 mm. The load-displacement curve was recorded automatically by a computer.

RESULT AND DISCUSSION

1. Load-Displacement Graph

From the test recording, the plots of the load versus displacement are given in Fig. 2 for Specimens #1-#3. For all the specimens, the load-displacement graphs can be clearly divided into two phases. First is the crack opening phase, in which the load increased from zero to the maximum value. All the specimens exhibit nearly the same linear elastic states. Second is the crack propagation phase. The loads of the three specimens decrease with the growth of delamination, but the load decrease of Specimen #1 is the fastest. Specimens #2 and #3 have a much smoother and more gradual descending curve. The obvious vertical line in the case of Specimens #2 and #3 marks the crack propagation (a-a_0) at 5 mm, 10 mm, … 100 mm, while the vertical line in the case of Specimen #1, represents 3 mm, 10 mm, … 100 mm, because of the unstable crack opening of Specimen #1.

2. Inter-laminar Fracture Toughness (G_I) Calculation

The critical load-displacement data for each crack opening interval were collected to calculate the interlaminar fracture toughness (G_I). The compliance calibration method [5] was applied to execute the calculation, which is defined in the following equation:

$$G_I = \frac{nP\delta}{2ba} \tag{1}$$

Where P is load, δ is load point displacement, b is specimen width, and a is the delamination length. The exponent n is obtained by the slope of log(a)-log(C) plot. That is:

$$n = \frac{\Delta(\log C)}{\Delta(\log a)} \tag{2}$$

Where C is the compliance of load and displacement, and it can be expressed as:

$$C = \frac{\delta}{P} \tag{3}$$

By applying Eqs. (2)-(3) in our case, the exponent n can be determined by the linear fitting of compliance vs. crack length in a full logarithmic scale. By reading from Fig. 3, one can find that the exponent n for Specimen #1 is 2.31952, for Specimen #2 is 2.21283, and for Specimen #3 is 2.14853.

With the values of exponent n and Eq. (1), the interlaminar fracture toughness G_I is calculated and listed in Table 1. From the table one can clearly see that the G_I values of specimen #3 are the highest, and it is more than 30% higher than that of specimen #1 in most cases. The percentage is larger with the growth of crack propagation. This phenomenon is thought to be the bridging effect from the through-thickness iron powder reinforcement.

2. Discussion

Fig. 4 illustrates the crack growth resistance curve (R-curve) for the three specimens, depicting G_I as a function of delamination length. All three specimens display an ascending trend.

For Specimen #1, this increasing resistance to delamination propagation is principally caused by the development of fiber bridging

Table 1. Calculated interlaminar fracture toughness G_I

	G_I (J/m^2)			Comparison	
	Specimen$^{\#}$ (G_{I1})	Specimen2$^{\#}$ (G_{I2})	Specimen3$^{\#}$ (G_{I3})	(G_{I2}-G_{I1})/G_{I1}*100%	(G_{I3}-G_{I1})/G_{I1}*100%
a_1	204.5	398.5	366.6	94.8	79.2
a_2	332.9	378.1	392.6	13.6	17.9
a_3	378.5	380.6	415.9	0.6	9.9
a_4	373.8	388.6	439.5	3.9	17.6
a_5	378.2	401.3	446.4	6.1	18.0
a_6	373.6	413.1	448.7	10.6	20.1
a_7	377.8	401.5	475.1	6.3	25.7
a_8	401.8	427.7	498.1	6.4	24.0
a_9	405.1	432.8	502.6	6.8	24.1
a_{10}	427.9	453.9	517.2	6.1	20.8
a_{11}	373.5	452.5	505.9	21.1	35.4
a_{12}	377.1	456.6	527.3	21.1	39.8
a_{13}	390.2	492.3	542.8	26.2	39.1
a_{14}	372.7	475.4	540.4	27.6	45.0
a_{15}	402.7	495.2	547.7	23.0	36.0
a_{16}	409.5	522.6	547.1	27.6	33.6
a_{17}	428.3	518.3	583.2	21.0	36.2
a_{18}	429.8	505.5	590.3	17.6	37.3
a_{19}	439.5	514.2	605.0	17.0	37.7
a_{20}	458.2	519.1	623.7	13.3	36.1

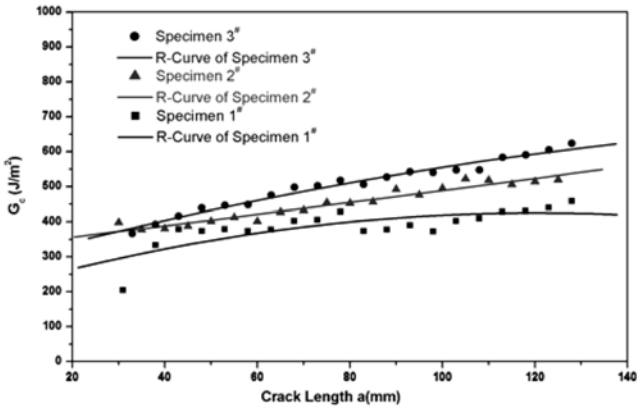

Fig. 4. R-curves for specimen #1, #2, #3.

between two unidirectional plies. This phenomenon was explained by Sørensen et al. [6] and Jacobsen et al. [7] in detail.

From Fig. 4, one can also see that the R- curves of Specimens #2 and #3 show linear increasing character. The inserted iron powder makes the crack propagation much more stable and regular. The R-curve of Specimen #1 changes into a flat line when the crack length is beyond 80 mm, which also verifies that the iron powder effectively burdens the opening force. A large part of the crack opening energy is used for iron-flake fracture and debonding between iron flakes and the matrix.

CONCLUSIONS

A new iron-powder reinforced carbon/epoxy laminated composite was developed. The fracture behaviors of this reinforced laminated composite were investigated in three kinds of DCB specimens. In the DCB test, the loads of the three specimens decreased with the growth of delamination, while the load decrease of Specimen #1 was the fastest. Specimens #2 and #3 had a much smoother and more gradual descending curve. The G_I values of specimen #3 were highest, which is more than 30% higher than that of specimen #1 in most cases. The percentage will be enlarged with the growth of crack propagation. The plotted crack growth resistance curve (R-curve) illustrates that all three specimens display an ascending trend. The R-curves of Specimens #2 and #3 show increasing linear characters, while that of Specimen #1 changes into a flat line. This identifies that the through-thickness iron powder effectively burdens the driving force for crack growth and provides a good stitching to the carbon/epoxy laminates.

REFERENCES

1. K. L. Rugg, B. N. Cox and R. Massabò, *Composites*, **Part A 33**, 177 (2002).
2. S. F. Hwang and B. C. Shen, *Comp. Sci. and Tech.*, **59**, 1861 (1999).
3. L. Chen, B. V. Sankar and P. G. Ifju, *Comp. Sci. and Tech.*, **62**, 1407 (2002).
4. H. T. Jang and W. S. Cha, *Korean J. Chem. Eng.*, **24**, 374 (2007).
5. ASTM D 5528-94a, Annual Book of ASTM Standard, Vol. 14.02, pp. 272-280.
6. B. F. Sørensen and T. K. Jacobsen, *Composites*, **Part A 29A**, 1443 (1998).
7. T. K. Jacobsen and B. F. Sørensen, *Composites*, **Part A 32**, 1 (2001).